SYNTHESIS OF MATERIAL COMPOSITE rGO-TIO$_2$ FROM COCONUT SHELLS BY SOL-GEL METHODS AS PHOTOCATALYST

Utiya Hikmah[*1], Diah Risma Yanti[1], David Lee Giant Axala[1], Erna Hastuti[1], Anton Prasetyo[2]

[1]Department of Physics, Faculty of Sciences and Technology, UIN Maulana Malik Ibrahim Malang, Indonesia
[2]Department of Chemistry, Faculty of Sciences and Technology, UIN Maulana Malik Ibrahim Malang, Indonesia
*utiyahikmah@fis.uin-malang.ac.id

ABSTRACT

The rGO- TiO$_2$ composite photocatalyst is receiving great attention because of its high performance. However the study of rGO- TiO$_2$ composite with sources of rGO material derived from using organic waste such as coconut shells is limited. In this study, the synthesis of nanocomposite rGO-TiO$_2$ was described with rGO obtained from coconut shells. The rGO samples are produced through the oxidation and reduction process. The transformation of graphene oxide into reduced graphene oxide was assisted by microwave irradiation. The obtained rGO was then composited with Titanium tetraisopropoxide (TTIP) by the sol-gel method. The composite of rGO- TiO$_2$ was characterized by XRD, FTIR, UV-Vis, and SEM. The photocatalytic performance of the rGO- TiO$_2$ composite was conducted on Methylene blue. The result shows that rGO- TiO$_2$ composite has a good photocatalytic performance with the highest number at 96%.

Keywords: rGO- TiO$_2$ composite; microwave irradiation; sol-gel method; photocatalyst

INTRODUCTION

The principle of photocatalysis is the use of photons to accelerate chemical reactions, allowing for the simultaneous acquisition of many benefits. This process can be done in low temperatures by conducting the reaction with photon energy instead of thermal energy. Furthermore, hazardous chemicals, which frequently exhibit limited biodegradability under ambient circumstances, can be broken down [1]. TiO$_2$ is a well-known photocatalyst substance used to degrade dyes due to its strong oxidizing power, suitable band gap energy, and resilience to chemical and photo corrosion. Though UV light makes up just 5% of the solar spectrum, TiO$_2$ has a vulnerability in that it is active in UV radiation due to its significant band gap energy of 3.2 eV. This suppresses the intrinsic photocatalytic properties, particularly in the visible light spectrum. The most recent innovation is the use of non-metal fillers or co-doped with additional compounds to enhance its photocatalytic activity [2-3]. One of the most recent innovations is the use of fillers derived from natural materials like graphene, activated carbon, and carbon nanotubes rather than metal ions.

Graphene is a 2D material that has a hexagonal lattice. Graphene has good thermal, electrical, mechanical, and optical properties and has a significant role in electronic applications, energy storage, battery electrodes, and photocatalysts [4]. Graphene has impressive qualities such as a large surface area (2630 m2g-1), its optical transmittance (97.7%), and good electrical conductivity. These characteristics make graphene a practical and effective co-catalyst. Moreover, graphene sheet has adjustable properties, has multiple functions, and shows outstanding performance in photocatalytic water splitting. The effectiveness of graphene, graphene oxide (GO), reduced Graphene Oxide (rGO), and their composites have been studied by several works applied to remove pollutants from aqueous solutions, including heavy metal ions, phenol, chlorophenol, photocatalysts, and microplastics [5-9]. The primary starting material for the manufacture of graphene is graphite. There are two types of graphite: natural graphite and synthetic graphite, which can be created by heat-induced hydrocarbon precursor graphitization. Because coconut shell charcoal has a high concentration of hydrocarbon compounds—roughly 74.3%—it can be used as a precursor to graphite[10].

Based on the abovemention explanation, in this research, the synthesis of rGO-TiO$_2$ composite was conducted using the sol-gel method. The rGO sample was produced from coconut shell and processed using the Hummer modification method and reduced using ascorbic acid (LAA), assisted by microwave irradiation (with time irradiation of 0, 10, 20, 30, and 40 minutes). Fast and uniform heating rates produced by microwave radiation can result in quick particle nucleation and development, which can shorten reaction times and save a significant amount of energy [11]. The rGO-TiO$_2$ composite then investigates the photocatalytic activity performance of the sample. The result shows that the sample has good photocatalytic activity.

MATERIALS AND METHODS

Synthesis of GO materials

The commercial coconut shell charcoal was crushed to obtain the powder of the coconut shell charcoal. The powder was then dispersed in 0.4 M HCl solution for 8 hours. The solution was then neutralized with DI water. Coconut shell charcoal powder (5 g) was added to the mixed acid solution of sulfuric acid (H$_2$SO$_4$) and 12.75 mL phosphoric acid (H$_3$PO$_4$). The solution was stirred, KMnO$_4$ (15 g) gradually, and the temperature of the mixture was controlled under 20°C, then added 230 mL of distilled water. The suspension was stirred for 40 minutes at 50°C with a stirring speed of 730 rpm, then adding 230 mL of DI water gradually. The hydrogen peroxide (5 mL) was used to stop the oxidation process. During this stage, the color of the mixture was changed from dark brown to yellow-brown. The mixture was washed with HCl and NaOH solution and then DI water to achieve a neutral solution. The sample was then dried at 60°C for 12 hours to obtain GO powder.\

Synthesis of rGO materials

The Graphite oxide powder (2 g) was dispersed into 268 ml of ethylene glycol and then proceeded with the sonication process for 2 hours. The reduction process used L-ascorbic acid (16 g) as a reduction agent and was assisted by microwave irradiation (Panasonic Microwave 2.45 MHz, 800 W). The microwave irradiation time was varied for 10, 20, 30, and 40 minutes using low mode. The reduction results were then filtered and washed using DI water and alcohol three times respectively. The sample was further dried for 12 hours at 60°C.

Synthesis of rGO/TiO$_2$ composites

Titanium tetraisopropoxide (TTIP) was mixed with Isopropanol and stirred for 30 minutes at room temperature. Then reduced graphene oxide (rGO) was added to the solution, added 14.72

mL of water, and stirred for 1 hour to form a gel. Further, the solution dried at 100°C for 12 hours, following the calcination process at 550°C for 4 hours with a heating rate of 1°C min^{-1}. Furthermore, the results of the synthesis of rGO-TiO$_2$ were characterized using XRD, FTIR, UV-Vis, SEM, and LCR-Meter. The rGO-TiO$_2$ composite was applied as a photocatalyst on methylene blue-containing solution.

RESULTS AND DISCUSSION

Synthesis of rGO-TiO$_2$ nanocomposites is carried out by mixing titanium tetraisopropoxide (TTIP) with rGO made from coconut shell charcoal, intending to increase the performance of obtaining samples as photocatalysts. The morphology of the sample was investigated using SEM, depicted in Figure 1. The rGO sample has a stack of a sheet as the characteristic of rGO material. Figure 1(b) shows the morphology of rGO-TiO$_2$ nanocomposites; the size and the geometry distribution of TiO$_2$ were not uniform.
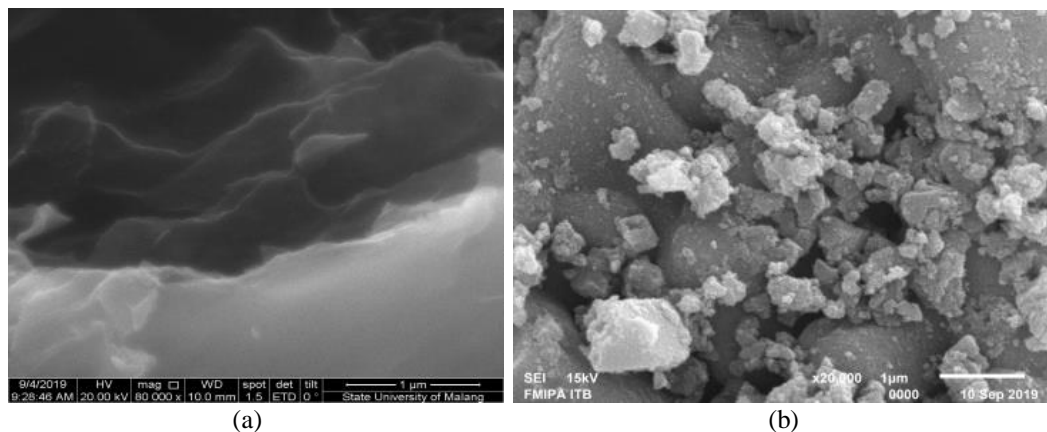

(a)   (b)

Figure 1. (a) The morphology of rGO and (b) rGO 40-TiO$_2$

The XRD pattern of the composite is displayed in Figure 2. Phase identification was analyzed by comparing experimental data with standard data reference of anatase phase TiO$_2$ (ICSD no 44882) and rutile phase (ICSD no 23697). The diffraction peaks in the XRD result are at $2\Theta =$ 25°, 37°, 48°, 53°, 62°, 68°, and 70°. Based on the appeared peak, the composite matched with the anatase phase of TiO$_2$. The rGO-TiO$_2$ nanocomposites have a diffraction pattern similar to pure titania and show the main peak at 25.15°. However, there are differences in the diffraction intensity of each sample; rGO TM-TiO$_2$ has the highest peak intensity of the diffraction pattern, which indicates a better crystallinity, followed by rGO 40m-TiO$_2$, rGO 10m-TiO$_2$, rGO 20m-TiO$_2$, and rGO 30m-TiO$_2$. It should be noted that the diffraction peak of rGO is at 24.5°; in this case, it is over-lapping by the main peak of the anatase TiO$_2$ at 25.3°[12], and it is hard to determine the differences in the quantity of the two phases since they have the same main peak position. Phase analysis was carried out using the Search-Match method using QualX software. The results in Table 1 describe the dominant phase in all samples as anatase for titania. But it is hard to clearly say that all samples are anatase because the FoM values are below 1. We assume that the presence of impurities in the form of rGO in the nanocomposite also affects the FoM values, just because there is a shift in the position of the peak 2θ in each experimental data.
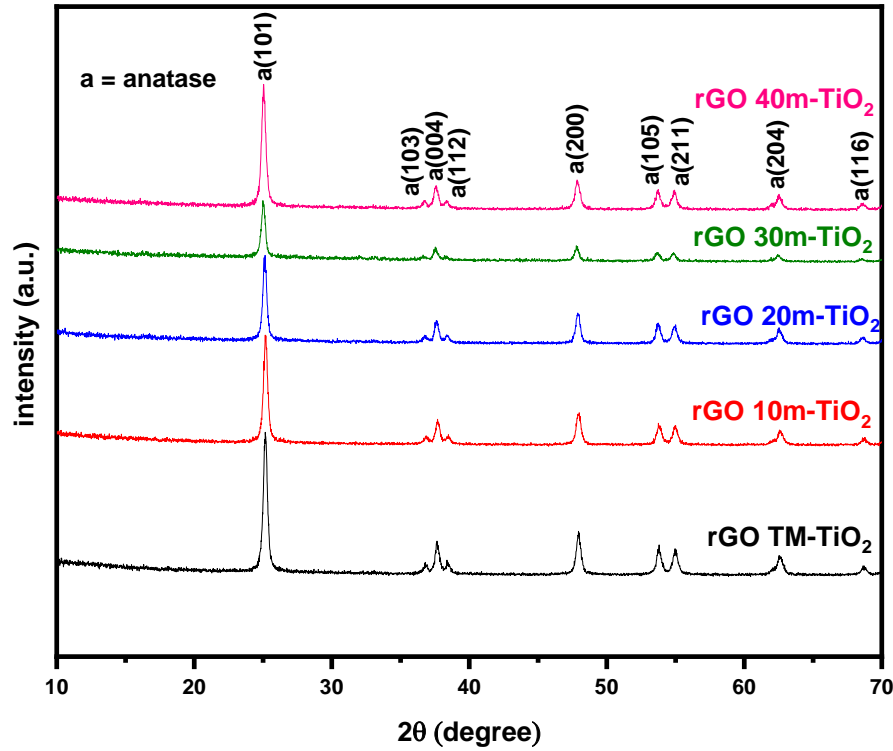
Figure 2. XRD pattern of rGO-TiO₂ composites

Table 1. The phase of the sample based on the Search-Match result

Samples	ICDD Number	Phase	FoM
rGO TM-TiO₂	00-900-8214	Anatas, TiO₂	0.91182
rGO 10m-TiO₂	00-900-8214	Anatas, TiO₂	0.90323
rGO 20m-TiO₂	00-900-8214	Anatas, TiO₂	0.82134
rGO 30m-TiO₂	00-900-8214	Anatas, TiO₂	0.79285
rGO 40m-TiO₂	00-900-8214	Anatas, TiO₂	0.921295

On the other hand, we utilize the Rietveld Method with the assistance of MAUD software. The refinement process was carried out using the material card with CIF code 1530151. The results after the refinement process are shown in Table 2; the dominant crystal structure formed is Tetragonal with the lattice length for a=b is 3.82Å, and c=9.49Å, and the lattice angle is α=β=γ=90°. The average crystal size value of the sample reaches 44 nm. The rutile phase and the brookite phase were hard to find because the quantity was very small or had the possibility of being amorphous, so there was overlapping on the diffraction peaks with the dominant phase.

Table 2. The crystal structure parameters of the sample based on the Rietveld refinement result

Samples	D (nm)	ε (10⁻³)	lattice a=b (Å)	lattice c (Å)	Rwp	Sig/GoF
rGO TM-TiO₂	43.81	1.082	3.777	9.496	14.66	0.934
rGO 10m-TiO₂	45.27	1.2133	3.786	9.515	15.97	0.867
rGO 20m-TiO₂	48.28	1.0462	3.785	9.519	17.30	0.922
rGO 30m-TiO₂	44.99	0.786	3.783	9.509	18.46	0.885
rGO 40m-TiO₂	41.66	1.0533	3.780	9.503	16.46	0.932

The FTIR result of the composite is shown in Figure 3. TiO_2 vibrations will create a strong absorption in the region of 400-1000 cm^{-1}, which indicates the presence of Ti-O-Ti bonds and vibrations of TiO2-rGO as a result of their chemical interaction[13]. In the area of 3200-3600 cm^{-1} is an O-H stretching vibration of H_2O molecules absorbed on the surface of TiO_2. The test results show the absorption in the area of 506-617 cm^{-1} and 3403-3436 cm^{-1}, which is the result of vibrations from Ti-O and Ti-OH. The absorption area of 1600 and 1800 cm-1 shows vibrations of C-O and C = C, which are carbon and aromatic functional groups that identify the presence of an rGO mixture.
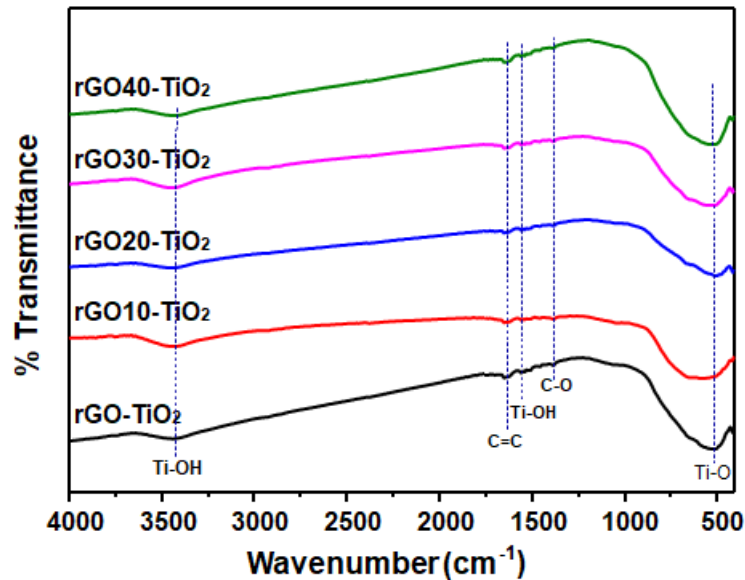
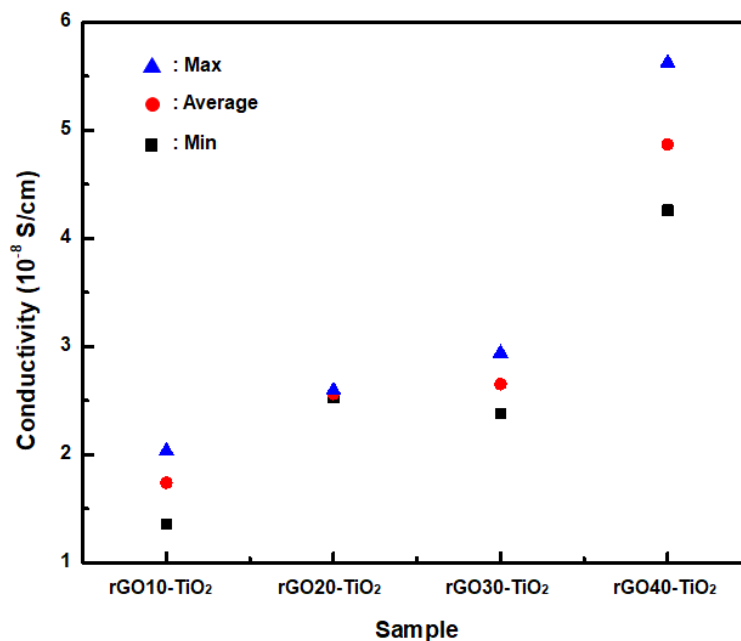**Figure 3.** FTIR spectra of rGO-TiO_2 composites

Figure 4. Electrical conductivity of rGO-TiO_2 composites

The electrical conductivity characterization of the sample was conducted using HIOKI LCR-Meter 3532-50 LCR HiTESTER. Data generated from this test are resistance and conductivity. The LCR-Meter test results were performed on rGO and rGO-TiO_2 Composite samples.

Theoretically, the value of conductivity is inversely proportional to resistance. The higher the resistance, the lower the conductivity, and vice versa. Figure 4. shows the electrical conductivity of rGO-TiO$_2$ composites. Variation in exposure time starts from 10 minutes, 20 minutes, 30 minutes, and 40 minutes. The composite samples were in pellet form. With the diameter and thickness of 1.029 cm and 0.124 cm, respectively. The results of the conductivity test for rGO-TiO$_2$ can be represented by a linear line; the higher the microwave exposure, the higher the conductivity value of the rGO-TiO$_2$ composite.

The LCR-Meter result shows that the longer the exposure, the greater the conductivity value, as shown in Figure 4. This is due to the influence of microwave exposure, which causes the heating process in the sample. An increased temperature causes motion between molecules so that the charged ions are close to uncharged molecules. Uncharged molecules that become charged by the influence of other charged particles are called dipoles. This process is called dipole induction. Molecules that can interact with microwaves are polar. The more dipoles formed, the more charged particles in the sample can affect the electrical conductivity. The ability of a sample to conduct electricity is called conductivity. The sample with the highest conductivity is rGO40-TiO$_2$, at about 5×10^{-8} S/cm.
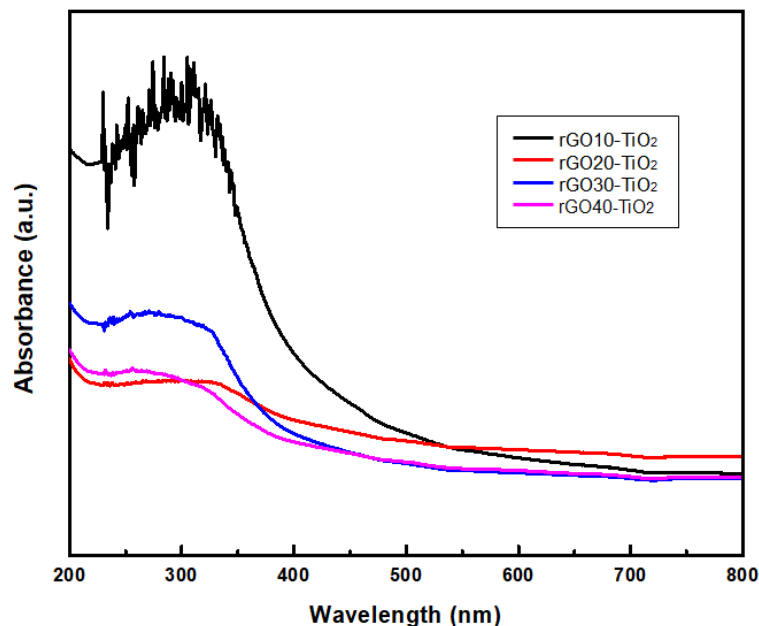

Figure 5. UV-Vis spectra of rGO-TiO$_2$ composites

Based on the UV-Vis result of the samples shown in Figure 3, the optical gap energy (Eg) can be obtained from the straight line intersection with the hυ axis of the Tauc plot [14]. The band gap energy value for rGO with microwave exposure for 40 minutes has the best band gap value at about 4.73 eV. The bandgap energies of graphene oxide and rGO-TiO2 composite The rGO-TiO$_2$ photocatalyst test was performed by using Methylene Blue as a pollutant solution. Before the RGO-TiO$_2$ composite photocatalyst activity test, several things need to be done first, including determining the maximum wavelength of methylene blue and making a standard methylene blue curve. Determination of the wavelength of methylene blue was carried out in the range of wavelengths from 400-800 nm using a Uv-Vis spectrophotometer. Methylene blue has a complementary color found at wavelengths between 610-750 nm.

The working principle of photocatalyst activity is that when light releases energy in the form of photons, the energy will be absorbed by the catalyst in the form of semiconductor material. Not all energy can be absorbed by the catalyst; only energy with a certain wavelength that is suitable for the semiconductor material used. Exposure to UV light gives photon energy to the

catalyst, thereby causing electron excitation or electron movement from the valence band to conduction and leaving holes in the valence band. The hole will interact with water (H_2O) to form hydroxyl radicals that are strong oxidizing agents. Strong oxidizing agents have large redox potential values, while the free electrons in the conduction band will interact with oxygen on the surface of the semiconductor and form a superoxide anion, which is a strong reducing agent. Superoxide anions then interact with water to form hydroxyl radicals. The hydroxyl radical will degrade methylene blue to produce products in the form of water, carbon dioxide, and other environmentally friendly compounds.

Based on the photocatalytic activity performance test, it can be explained that the $rGO-TiO_2$ photocatalyst is effectively used to degrade methylene blue. In this study, a photocatalyst test was conducted in 30 minutes. Photodegradation in the 30 minutes has achieved good catalytic performance activity, with percent degradation ranging from 82-96%. The highest MB degradation is 96.03%, reached by $rGO30-TiO_2$. The result of the photocatalytic activity performance is described in Table 3 and Figure 6.

Table 3. The photocatalytic performance of $rGO-TiO_2$ composites

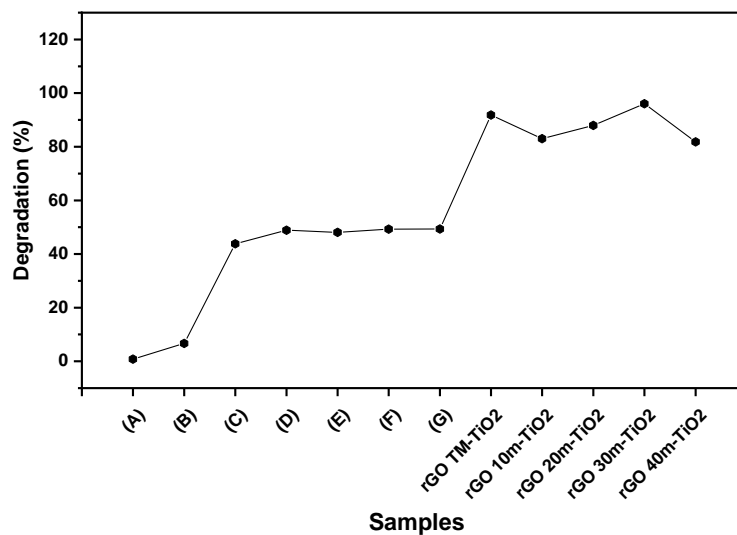| Sample	Degradation (%)
No Light No Catalyst (A)	0.83
With Light Without A Catalyst (B)	6.65
No Light With Catalyst $rGOTM-TiO_2$ (C)	43.84
No Light With Catalyst $rGO10-TiO_2$ (D)	48.85
No Light With Catalyst $rGO20-TiO_2$ (E)	48.09
No Light With Catalyst $rGO30-TiO_2$ (F)	49.28
No Light With Catalyst $rGO40-TiO_2$ (G)	49.34
$rGOTM-TiO_2$	91.81
$rGO10-TiO_2$	82.98
$rGO20-TiO_2$	87.97
$rGO30-TiO_2$	96.03
$rGO40-TiO_2$	81.82

Figure 6. The photocatalytic performance of $rGO-TiO_2$ composites

Figure 6. shows that the addition of rGO to TiO$_2$ further increases its photodegradation activity because rGO or graphene can maximize the absorption of light. Increased light absorption results in better photocatalyst activity.

CONCLUSION

The nanocomposite of rGO-TiO$_2$ has been successfully performed by the sol-gel method. The structure and morphology of rGO-TiO$_2$ were confirmed by ATR-FTIR, XRD, UV-Vis, and SEM results. The synthesized rGO was assisted by microwave irradiation with LAA as a reducing agent. The band gap energy value for rGO with microwave exposure for 40 minutes has the best band gap value at about 4.73 eV. The surface morphology of the RGO from the coconut shell shows the presence of peeling sheets, showing the formation of RGO. Microwave exposure affects rGO. The highest sample conductivity was found in rGO with an exposure time of 40 minutes. Synthesized rGO-TiO$_2$ nanocomposite samples can be used to degrade pollutant solutions with a degradation time of 30 minutes, obtaining degradation results between 82.9% and 96.03%.

REFERENCE

1   Granone, L. I., Sieland, F., Zheng, N., Dillert, R., & Bahnemann, D. W. 2018. Photocatalytic conversion of biomass into valuable products: a meaningful approach?. *Green chemistry, 20*(6), 1169-1192.
2   Deshmukh, S. P., Kale, D. P., Devyani, P., Kar, S., Shirsath, S. R., Bhanvase, B. A., Saharan, V. K., & Sonawane, S. H. 2020. Ultrasound assisted preparation of GO/TiO nanocomposite for effective photocatalytic degradation of methylene blue under sunlight. *Nano-Structures & Nano-Objects, 21*, 100407.
3   Padmanabhan, N. T., Thomas, N., Louis, J., Mathew, D. T., Ganguly, P., John, H., & Pilla, S. C. 2021. Graphene coupled TiO2 photocatalysts for environmental applications: A review. *Chemosphere, 271*, 129506.
4   Iskandar, F., Hikmah, U., Stavilla E., & Aimon A.H. 2017. Microwave-assisted reduction method under nitrogen atmosphere for synthesis and electrical conductivity improvement of reduced graphene oxide (rGO). *RSC Advances, 7*(83), 52391-52397.
5   Nada, A. A., McKay, G., & Abdala, A. 2020. Recent advances in applications of hybrid graphene materials for metals removal from wastewater. *Nanomaterials, 10* (3), 595.
6   Vineh, M. B., Saboury, A.A, Poostchi, A. A., Rashidi, A. M., & Parivar, K. 2018. Stability and activity improvement of horseradish peroxidase by covalent immobilization on functionalized reduced graphene oxide and biodegradation of high phenol concentration. *Int. J. Biol. Macromol, 106*, 1314–1322.
7   Wei, D.,Zhao, C., Khan, A., Sun, L., Ji, Y., Ai, Y., & Wang, X. 2019. Sorption mechanism and dynamic behavior of graphene oxide as an effective adsorbent for the removal of chlorophenol based environmental-hormones: a DFT and MD simulation study. *Chem. Eng. J., 375,* 121964.
8   Liang, Q., Luo, H., Geng, J., & Chen, J. 2018. Facile one-pot preparation of nitrogen-doped ultra-light graphene oxide aerogel and its prominent adsorption performance of Cr (VI). *Chem. Eng. J., 338*, 62–71.
9   C. Sun, Z. Wang, L. Chen, & F. Li, F. 2020. Fabrication of robust and compressive chitin and graphene oxide sponges for removal of microplastics with different functional groups. *Chem. Eng. J., 393*, 124796.
10 Sujiono, E. H., & Zurnansyah, Z. D. 2020. Graphene oxide-based coconut shell waste: synthesis by modified Hummers method and characterization. Heliyon, 6 (8), e04568.
11 Omar, F. S., Nay Ming, H., Hafiz, S. M., & Ngee, L. H. (2014). Microwave synthesis of zinc oxide/reduced graphene oxide hybrid for adsorption-photocatalysis application. *International Journal of Photoenergy, 2014.*
12 Thakur, A., Kumar, S., & Rangra, V. S. 2015. Synthesis of reduced graphene oxide (rGO) via chemical reduction. *In AIP Conference Proceedings, 1661*(1).

13 Martínez, M. R., Álvarez, M. A., Ramón, M. V. L., Quesada, G. C., Utrilla, J. R., & Polo, M. S. 2020. Hydrothermal synthesis of rGO-TiO2 composites as high-performance UV photocatalysts for ethylparaben degradation. *Catalysts, 10*(5), 520.

14 AlShammari, A. S., Halim, M. M., Yam, F. K., & Kaus, N. H. M. 2020. Effect of precursor concentration on the performance of UV photodetector using TiO2/reduced graphene oxide (rGO) nanocomposite. *Results in Physics, 1*9, 103630.